Molecular Crystals and Liquid Crystals Incorporating Nonlinear Optics
Publication details, including instructions for authors and subscription information:
http://www.tandfonline.com/loi/gmcl17

Nonlinear Diffraction of CW-Laserbeams by Spatial Selfphase-Modulation in Nematic Liquid Crystals

H. J. Eichler [a] , R. Macdonald [a] & C. Dettmann [a]
[a] Optisches Institut, Technische Universität Berlin, Straße des 17, Juni, 1000, Berlin 2, FRGermany
Version of record first published: 04 Oct 2006.

To cite this article: H. J. Eichler , R. Macdonald & C. Dettmann (1989): Nonlinear Diffraction of CW-Laserbeams by Spatial Selfphase-Modulation in Nematic Liquid Crystals, Molecular Crystals and Liquid Crystals Incorporating Nonlinear Optics, 174:1, 153-168

To link to this article: http://dx.doi.org/10.1080/00268948908042701

Mol. Cryst. Liq. Cryst., 1989, Vol. 174, pp. 153–168
Reprints available directly from the publisher
Photocopying permitted by license only

Printed in the United States of America

Nonlinear Diffraction of CW-Laserbeams by Spatial Selfphase-Modulation in Nematic Liquid Crystals

H. J. EICHLER, R. MACDONALD and C. DETTMANN

Optisches Institut, Technische Universität Berlin Straße des 17.Juni, 1000 Berlin 2, FRGermany

(*Received March 6, 1989*)

Optical nonlinearities in nematic liquid crystals lead to strong self-defocussing and nonlinear diffraction effects with low power laser intensities of some hundred Watts/cm^2. We describe these diffraction effects by expanding the transversally modulated intensity behind the sample into gaussian beams. Using in addition a simple model of light-induced reorientation of nematic liquid crystals as nonlinear mechanism, we get good agreement between theory and self-diffraction experiments, which have been done in the liquid crystal 5CB.

I. INTRODUCTION

Propagation of laserbeams through optically nonlinear materials can result in distortions of the beams, well-known as self-focussing-, self-defocussing- or self-diffraction-effects. In many materials detailed studies of these effects are more or less complex because thick samples established in weak optical nonlinearities are needed and often give reason for both, dispersive and absorptive effects.[1]

Nematic liquid crystals, however, show strong nonresonant dispersive optical nonlinearities, and strong self-defocussing or self-diffraction can be achieved in thin films of some tens to some hundreds μm's thickness even with low power laser intensities of a few hundred W/cm^2.[2] Since certain nematics, as for example the cyano-biphenyls, are furthermore nearly nonabsorptive over the whole visible spectral range,[3] such nonlinear films are ideal objects for the analysis of purely dispersive self-diffraction effects.

Self-diffraction effects in liquid crystals have been investigated experimentally in a more phenomenological way[2,11] or theoretical without really quantitative comparisons to experiments (and for one special case)[8] until now.

In the following we calculate the self-diffraction of a gaussian laserbeam by a light-induced gaussian phasemodulation. Calculation is done by expanding the spatial intensity distribution behind the film in terms of gaussian beams. Experiments have been performed in the nematic liquid crystal 5CB (pentyl-cyanobi-

phenyl), so we start with a short review of the theory of light-induced reorientation of liquid crystals as the relevant nonlinear mechanism. Comparison between experimental data and theory is given in the last section.

II. LIGHT-INDUCED REORIENTATION OF NEMATIC LIQUID CRYSTALS

Unusual strong optical nonlinearities can be obtained in nematic liquid crystals by light-induced reorientation of the nematic's director. Light-intensities needed for this effect are low and can be realized easily even with cw-lasers. Nematics are optically uniaxial anisotropic, the optical axis lying parallel to the director, which describes the local preferred direction of alignment of the liquid crystal molecules. So reorientation of the director by external electric or magnetic fields is always accompanied by a reorientation of the optical axis. In the case of an incident linearly polarized laserbeam on a homeotropic aligned liquid crystal as depicted in Figure 1, the optical field yields in a reorientation of the director **L** which leads to changes in the extraordinary refractive index. The reorientation can be described by an angle Θ, which is obtained by a torque-balance[4]

$$\gamma \frac{\delta\Theta}{\delta t} - K\Delta\Theta - \frac{1}{2}\epsilon_o\epsilon_a E_{op}^2 \sin[2(\Theta + \beta)] = 0 \tag{1}$$

where K is the elastic-constant (in a one constant approximation), γ the effective viscosity, $\epsilon_a = \epsilon_\parallel - \epsilon_\perp$ the optical anisotropy and β the angle between the wavevector and the initial alignment. Changes in the refractive index established by this reorientation are given by

$$\delta n = n_e(\Theta + \beta) - n_e(\beta) \tag{2}$$

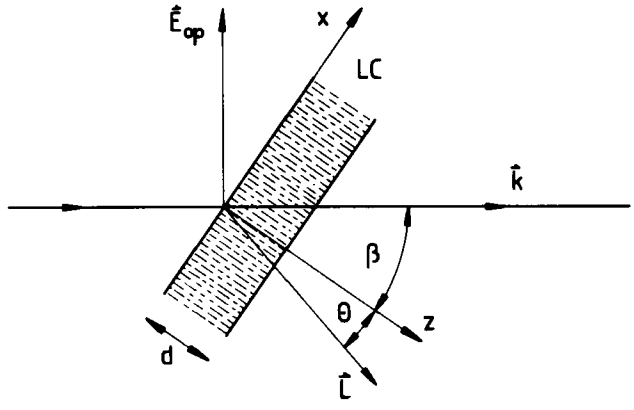

FIGURE 1 Scheme of optical reorientation of a homeotropically aligned liquid crystal. $\mathbf{E}_{op}$: Optical field, **k**: Wavevector, **L**: Director, d: Film-thickness, β: Initial orientation, Θ: Reorientation-angle.

where

$$n_e(\vartheta) = n_\perp n_\parallel (n_\parallel^2 \cos^2\vartheta + n_\perp^2 \sin^2\vartheta)^{-1/2} \tag{3}$$

with $\vartheta = \Theta + \beta$ resp. $\vartheta = \beta$, $n_\perp = \sqrt{\epsilon_\perp}$, $n_\parallel = \sqrt{\epsilon_\parallel}$.

If we assume e.g. $\beta \approx 0$ and we have no reorientation (i.e. $\Theta = 0$) at low intensities one gets $n_e = n_\perp$. At higher intensities the director can be reorientated to nearly $\Theta = 90$ deg and $n_e \approx n_\parallel$. So the induced change of n_e could be in the order of the full optical anisotropy $\delta n \approx n_\parallel - n_\perp \approx 0.1$, which is some orders of magnitude more than in most usual nonlinear materials.

To calculate the locally light-induced change of the refractive index in presence of an optical field one has to solve the nonlinear Equation 1, which is in general not possible by analytical means. Therefore we treat some special cases giving approximate solutions for the spatial distribution and dynamics of the reorientation angle.

Spatial reorientation distribution and threshold ($\Theta \leq 0.6$, $\beta = 0$, $\partial\Theta/\partial t = 0$)

With a linearized approximation Equation 1 for the spatial director-deformation in steady state and the case of normal incidence ($\beta = 0$) simplifies to

$$K \Delta\Theta + \epsilon_o \epsilon_a E_{op}^2 \Theta = 0 \tag{4}$$

For axially symmetric laserbeams this equation can be solved under the boundary conditions $\Theta(z = 0) = \Theta(z = d) = 0$ by[5]

$$\Theta(\rho,z) = R(\rho) \sin \frac{\pi}{d} z \tag{5}$$

where d denotes the film-thickness and $R(\rho)$ obeys the equation

$$\frac{\delta^2 R}{\delta\rho^2} + \frac{1}{\rho}\frac{\delta R}{\delta p} + \left(\frac{\epsilon_o \epsilon_a}{K} E_{op}^2 - \left(\frac{\pi}{d}\right)^2\right) R = 0 \tag{6}$$

Assuming the laserbeam to be of the form

$$E_{op}^2(\rho) = \begin{cases} E_{op}^2 & \rho \leq w_o \\ 0 & \rho > w_o \end{cases} \tag{7}$$

where w_o denotes an effective beam radius, we get a nontrivial solution of Equation 6 under the boundary conditions $R(\rho = 0) = 1$, $R(\rho \to \infty) = 0$, $R'(\rho = 0) = 0$ with

$$R(\rho) = \begin{cases} I_o(\lambda\rho) & \rho \leq w_o \\ aK_o(\mu\rho) & \rho > w_o \end{cases} \tag{8}$$

where l_o and K_o are modified Bessel- and Hankel-functions of zeroth-order, resp.[6], and $\lambda^2 = \epsilon_o\epsilon_a K^{-1}E_{op}^2 - (\pi/d)^2$, $\mu^2 = (\pi/d)^2$. Solutions of physical meaning are only obtained with $\lambda \geq 0$, which implies the existence of a certain threshold. The threshold for optical fields of finite spot-size can be calculated by an adaptation-condition[5] of Equation 8 and the solution of this adaptation-condition leads to a modified threshold

$$E_{th}^2 = E_F^2 (b^2 \kappa^{2(m-1)} + 1) \tag{9}$$

where $E_F^2 = (\pi/d)^2 K/(\epsilon_o\epsilon_a)$ is the well-known Freedericks-threshold, $\kappa = \mu w_o$ and $b = 1.43$, $m = 0.24$. In the case of plane waves, i.e., $\kappa \to \infty$, we have the transition $E_{th}^2 \to E_F^2$.

As has been pointed out by Khoo *et al.*[7] the radial distribution $R(\rho)$ of the reorientation angle Θ as e.g. given in Equation 8 is not gaussian and the reorientation-profile's waist is differing from the incident beam-waist, depending on the ratio of beam-waist to film-thickness. This is due to strong interactions between the nematic molecules and shows the influence of the correlation-length which is determined by the film-thickness. However, the induced lens as given by Equation 8 together with Equation 2 and Equation 3 can be approximated well by a gaussian profile in the small angle limits (i.e. $\Theta_o \leq 40$ deg) as it is shown in Figure 2. The lens-diameter is also differing from the beam-diameter and can be greater (in the case $w_o < d$) or smaller (for $w_o > d$).

Dynamics and amplitude ($w_o \to \infty$)

Though the phase-profile and the threshold can be calculated with the linearized Equation 4, the reorientation-amplitude and its dependence upon light-intensity

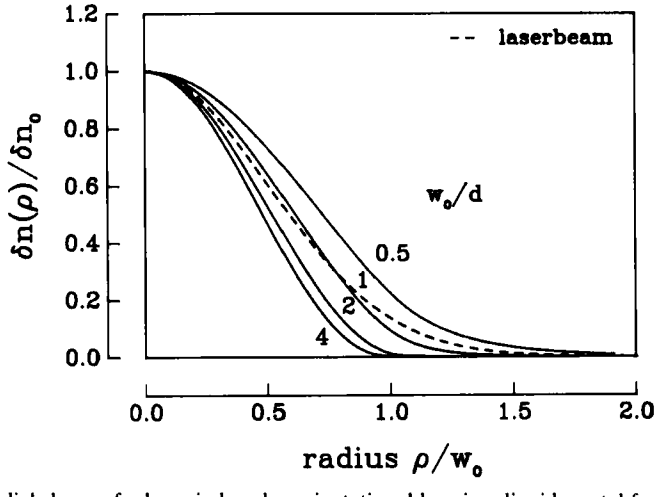

FIGURE 2 Radial shape of a laser-induced reorientational lens in a liquid crystal for different ratios w_o/d. w_o: Input beam radius, d: Film-thickness, $\delta n_o = 0{,}05$.

cannot be determined with the small-angle approximation used so far. Therefore the dynamics of reorientation (and also the amplitude in the steady state) are calculated in the following in a plane wave approximation. An approximate solution of Equation 1 for this case under the boundary conditions $\Theta(z = 0) = \Theta(z = d) = 0$ can be written as

$$\Theta(z,t) = \Theta_m(t) \sin \pi/dz \tag{10}$$

where $\Theta_m(t)$ is the amplitude of reorientation at $z = d/2$ and obeys the equation

$$\frac{\delta\Theta_m}{\delta t} + \frac{K}{\gamma}\left(\frac{\pi}{d}\right)^2 \Theta_m - \frac{\epsilon_o\epsilon_a}{2\gamma}E_{op}^2 \sin[2(\Theta_m + \beta)] = 0 \tag{11}$$

Solutions for Equation 11 are discussed in the following for a stepwise optical excitation, i.e.

$$E_{op}^2(t) = \begin{cases} E_{op}^2 & t \geq 0 \\ 0 & t < 0 \end{cases} \tag{12}$$

A numerical solution for this case is shown in Figure 3a and Figure 3b. The dynamics of reorientation depend on one hand on laser-intensity (see Figure 3a), on the other hand on the angle of incidence (see Figure 3b).

β mainly determines the 'delay-time' between the optical excitation and the beginning of the reorientation process, whereas the intensity determines the rise-time and also the amplitude in the steady state. The amplitude in the steady state can also be obtained from Equation 11 by setting $\delta\Theta_m/\delta t = 0$. If we denote $\Theta_m = \Theta_m(t \to \infty)$, we get with Equation 10

$$\left(\frac{E_{op}}{E_{th}}\right)^2 = \frac{2\,\Theta_m}{\sin[2(\Theta_m + \beta)]} \tag{13}$$

The inverse function of Equation 13 describes the amplitude of reorientation depending on laser intensity and β.

Small-angle dynamics ($\Theta \leq 0.6$, $w_o \to \infty$)

Some of our experiments can be simply explained with a small angle approximation of Equation 11 which should be discussed finally. For small amplitudes $\Theta_m(t)$ we can write $\sin[2(\Theta_m + \beta)] \approx 2\Theta_m \cos 2\beta + \sin 2\beta$ which leads to

$$\frac{\delta\Theta_m}{\delta t} + \gamma^{-1}\left(K\left(\frac{\pi}{d}\right)^2 - \epsilon_o\epsilon_a E_{op}^2 \cos 2\beta\right) = \frac{\epsilon_o\epsilon_a E_{op}^2 \sin 2\beta}{2\gamma} \tag{14}$$

with the solution

$$\Theta_m(t) = \frac{\epsilon_o\epsilon_a}{2\gamma} \sin 2\beta \int_{-\infty}^{t} E_{op}^2(t) \exp\left[-\frac{(t - t')}{\tau}\right] dt' \tag{15}$$

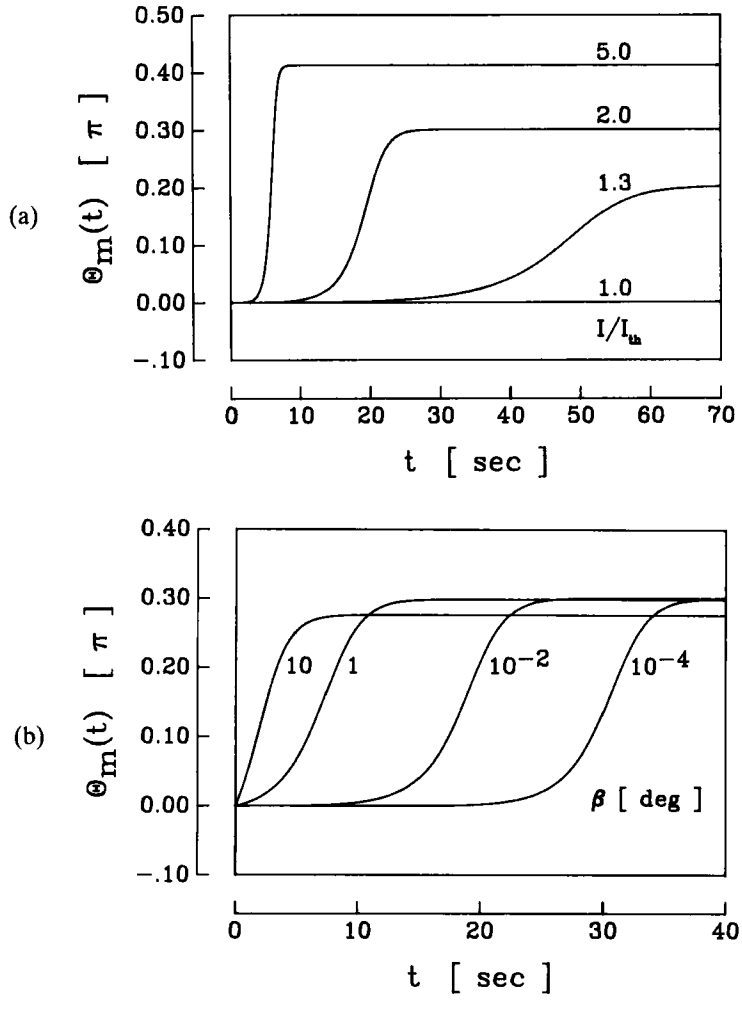

FIGURE 3 Amplitude of the reorientation-angle vs. time for a stepwise excitation at $t = 0$ for different input-intensities (a) and with different starting-angles β (b). In case (a) we chose typically values as I_{th} = 300W/cm², β = 10^{-2} deg, γ = 0,02kg/ms. In case (b) we take I/I_{th} = 2, I_{th} = 300W/cm², γ = 0,02kg/ms.

where

$$\tau = \frac{\gamma}{\epsilon_o \epsilon_a (E_F - E_{op}^2 \cos 2\beta)} \tag{16}$$

and

$$E_F^2 = \left(\frac{\pi}{d}\right)^2 \frac{K}{\epsilon_o \epsilon_a} \tag{17}$$

For a stepwise optical excitation as described in Equation 12, Equation 15 can be integrated to give

$$\Theta_m(t) = \frac{\epsilon_o \epsilon_a}{2\gamma} \sin 2\beta \; E_{op}^2 \; \tau \left(1 - \exp\left[-\frac{t}{\tau}\right]\right) \tag{18}$$

where τ can be interpreted as the time-constant for optical reorientation build-up. Notice that in the case of finite spot-size the time constant as given in Equation 16 should be modified by substituting $E_F^2 \rightarrow E_{th}^2$ as shown in Equation 9. It should also be noted here, that τ can be positive or negative, depending on whether E_{op}^2 cos 2β is smaller or larger than threshold-intensity. So the dynamics as given above are quite different for these two cases.

The reorientation decay after switching off the laser is also described by Equation 16 by simply setting $E_{op}^2 = 0$, resulting in a decay-time which is determined by the elastic behaviour and the viscosity of the liquid crystal.

III. DIFFRACTION AT LIGHT-INDUCED GAUSSIAN LENSES

Consider a gaussian laserbeam slightly focussed on a thin nonlinear film. In the case of intensity-depending refractive index as described in chapter II, the phase of that beam would be modulated transversally (self-phase-modulation). The resulting intensity-distribution on a screen placed at a distance Z behind the sample can be calculated with Kirchhoff's diffraction-theory[8] for instance, or with the optics of Gaussian beams.[9] In the geometric-optics approximation the only effect of the nonlinear refractive index is to produce a phase-shift, which varies across the beam profile. Because we have Gaussian beams and (more or less) Gaussian phase-profiles, the method of Gaussian optics seems to be quite accurate and leads easily to numerical results indeed. For the first time we obtained quantitative agreement of calculated and observed self-defocussing effects in thin liquid crystal films.

Starting point is an incident Gaussian laserbeam on the film

$$I(\rho) = I_o \exp\left(-\frac{2\rho^2}{w_o^2}\right) \tag{19}$$

where we assumed the sample to be placed in the beam-waist w_o and I_o denotes the on-axis intensity. In liquid crystal films the laser-induced phase shift can also be assumed to have a gaussian profile but with a quite different profile-waist, as has been shown in the last chapter. So we write

$$\partial\Psi(\rho) = \partial\Psi_o \exp\left(-\frac{2\rho^2}{(fw_o)^2}\right) \tag{20}$$

where $\partial\Psi_o$ denotes the on-axis phase-shift and f is the ratio of the profile-waist to the incident beam-waist. The phase amplitude is given by $\partial\Psi_o = kd\partial n_o$ where k is the wave-number, d the film-thickness and ∂n_o denotes the induced change of

the refractive-index on the beam-axis. ∂n_o (and also $\partial\Psi_o$) depends on the incident laser-intensity in general.

So the optical field just behind the film can be written as

$$E_{op}(\rho, z = 0) = E_o \exp\left[\left(-\frac{\rho^2}{w_o^2}\right) + i\,\partial\Psi_o \exp\left(-\frac{2\rho^2}{(fw_o)^2}\right)\right] \tag{21}$$

which can be expanded into

$$E_{op}(\rho, z = 0) = E_o \sum_{m=0}^{\infty} \frac{(i\partial\Psi_o)^m}{m!} \exp\left[-\frac{\rho^2}{w_{mo}^2}\right] \tag{22}$$

where $w_{mo}^2 = w_o^2/(2m/f^2 + 1)$. Equation 22 describes the modulated field by a sum of Gaussian beams of decreasing beam-waists w_{mo} as depicted in Figure 4. Using Gaussian optics the optical field at any point behind the sample can be expanded in the same way to give

$$E(\rho,z) = E_o \sum_{m=0}^{\infty} \frac{(i\partial\Psi_o)^m}{m!} \frac{w_{mo}}{w_m} \exp\left[-\frac{\rho^2}{w_m^2} - \frac{k\rho^2}{i2R_m} - i\Phi_m\right] \tag{23}$$

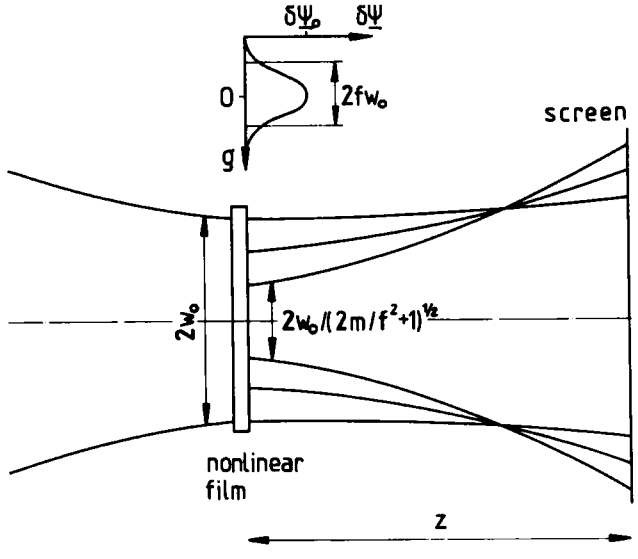

FIGURE 4 Diffraction of a gaussian laser-beam at an induced gaussian lens. The field behind the nonlinear film can be expanded into a sum of gaussian beams with decreasing beam-waists.

with

$$w_m^2(z) = w_{mo}^2 (1 + 1/F_m^2) \tag{24a}$$

$$R_m(z) = z (1 + F_m^2) \tag{24b}$$

$$\Phi_m(z) = \text{arctg}\,(1/F_m) \tag{24c}$$

and $F_m = \pi w_{mo}^2/\lambda z$. For small Fresnel-numbers $\pi w_o^2/\lambda z \ll 1$ we have $\pi w_o^2/(2m/f^2 + 1)\lambda Z \ll 1$ because $2m/f^2 > 0$. So we can approximate

$$w_m^2(z) = w_o^2 (2m/f^2 + 1)/F_o^2 \tag{25a}$$

$$R_m(z) \approx z \tag{25b}$$

$$\Phi_m(z) \approx (2m/f^2 + 1)\frac{\pi}{2} \tag{25c}$$

where $F_o = \pi w_o^2/\lambda z$ and Equation 23 can be rewritten to give

$$E(\rho,z) = E_o F_o \exp\left[-i\frac{k\rho^2}{2z}\right] \sum_{m=0}^{\infty} \frac{(i\partial\Psi_o)_m}{m!(2m/f^2 + 1)} \exp\left[-\frac{\rho^2 F_o^2}{w_o^2(2m/f^2 + 1)}\right] \tag{26}$$

As can be seen by this equation, the optical field can be expressed in terms of Fresnel-integrals for the special case $f = 1$ and $\rho = 0$.[9] In Figure 5 we calculated the transversal intensity-distribution on a screen with respect to the different phase-shifts by using Equation 26. In the case $\partial\Psi_o = 0$ we have the undistorted gaussian laser-beam, with $\partial\Psi_o = 2\pi$ or $\partial\Psi_o = 4\pi$ we have defocussing effects and one or two diffraction-rings appear respectively. The influence of the on-axis phase-shift upon the diffraction pattern is also shown in Figure 6 in more detail. In Figure 6a the normalized radial intensity-distribution shows the distortion of the incident laser-beam and the occurrence of side-wings with increasing on-axis phase-shift. In Figure 6b it is shown that the number of appearing diffraction-rings N is related to the induced phase-shift by $N = \partial\Psi_o/2\pi$. This has been proved by our model in the limits of $N \leq 6$ and $f \leq 2$ so far. It is obvious that for much larger lens-profiles (compared to the lasers beam-waist) this relation must be violated (e.g. if the gaussian distribution of the phase-shift can be approximated by a parabolic lens). In Figure 7 we have calculated the on-axis intensity as a function of the induced phase-shift for 3 different phase-profile diameters expressed by the factor f. The on-axis intensity is oscillating with a period of 2π with increasing $\partial\Psi_o$. The ratio between the on-axis intensity and the diffracted intensity is determined by the factor f.

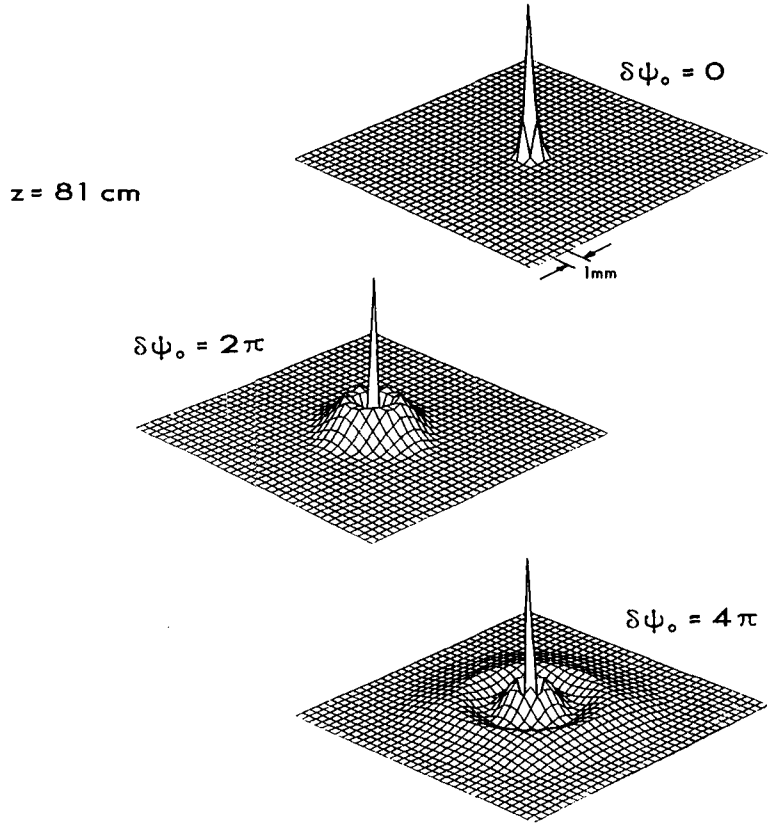

FIGURE 5 Calculated (normalized) transversal intensity-distribution on a screen placed at z behind the sample for a laser-beam diffracted at a gaussian lens. $\delta\Psi_o$ is the induced on-axis phase shift.

IV. EXPERIMENTS

A simple arrangement for the investigation and analysis of self-diffraction effects is depicted schematically in Figure 8. The linear polarized beam of a cw-argon-laser is focussed ($1/e^2$—radius $w_o = 170\ \mu m$) on a thin film of the liquid crystal 5CB (pentyl-cyano-biphenyl) to leave the nonlinear film (thickness $d = 120\ \mu m$) with strong diffraction effects. The resulting diffraction pattern can be observed on a screen for instance. As pointed out above, the intensity pattern consists of axially symmetric rings, where the number of rings depends on the incident laser-intensity, but also on film-thickness or the angle of incidence β. In Figure 9 we compare the number of observed diffraction-rings with the calculated induced on-axis phase-shift using the relation $N = \partial\Psi_o/2\pi$ as has been suggested in the last chapter, N and $\partial\Psi_o$ are depicted as a function of laser-intensity and for three different angles β. A good agreement between theory and experimental data is achieved if we assume an effective phase-shift (integrated over film-thickness) somewhat smaller (factor 0.8 for $\beta = 0$ and 10 deg and 0.9 for $\beta = 45$ deg) than

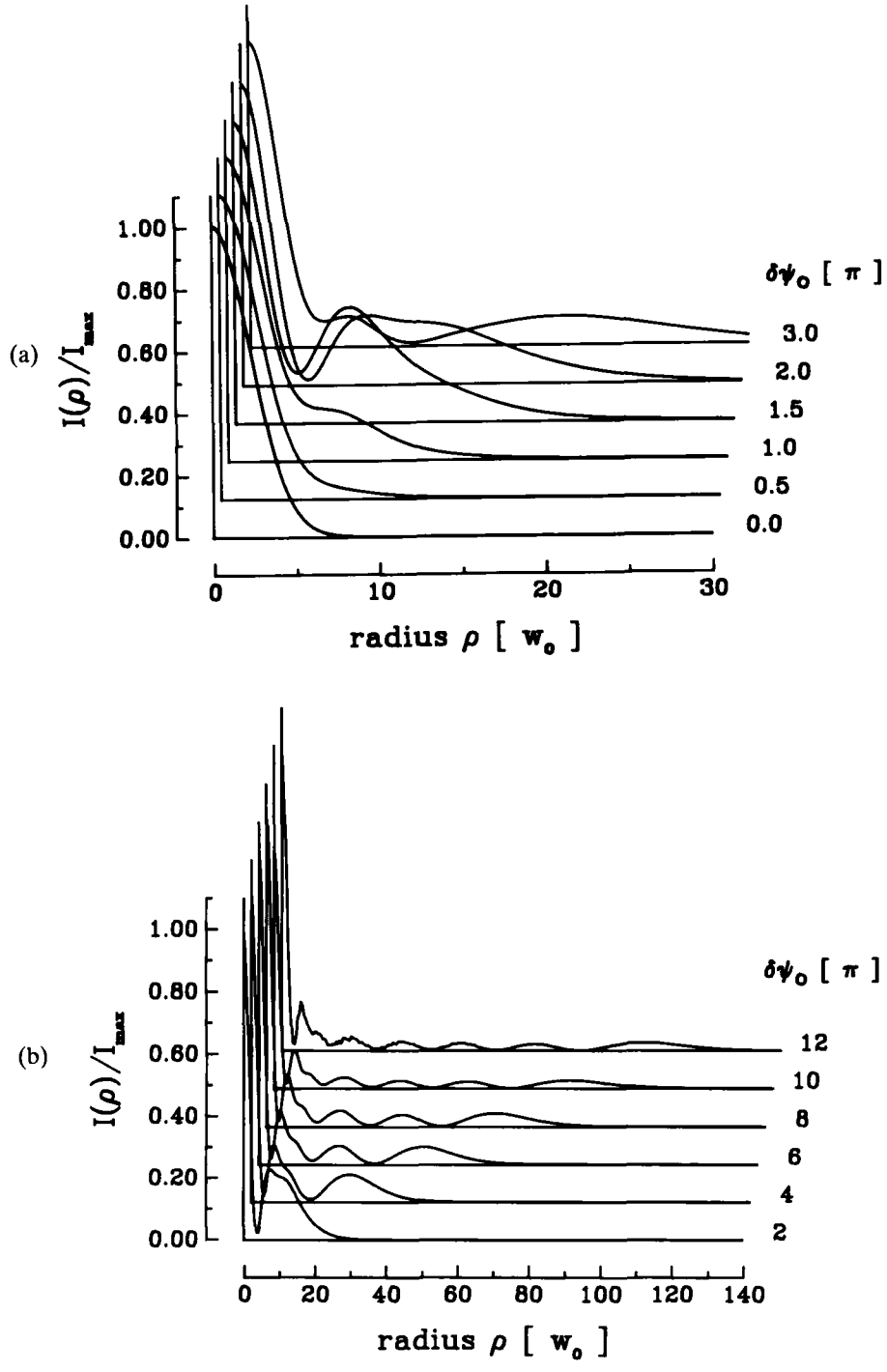

FIGURE 6 Normalized radial intensity-distribution behind the nonlinear film with increasing on-axis phase-shift $\delta\psi_o$.

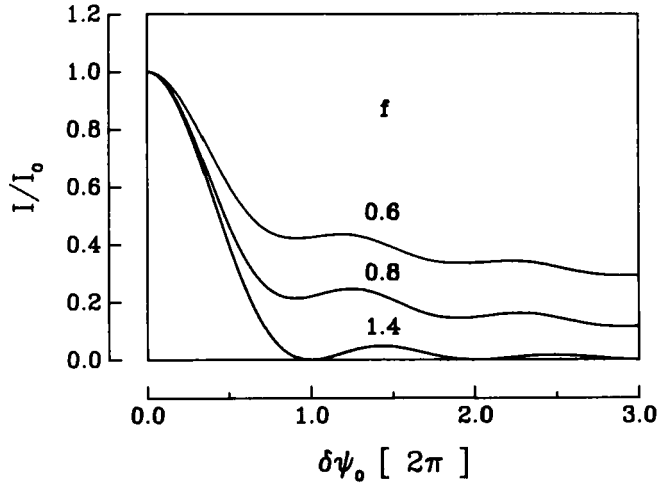

FIGURE 7 Normalized on-axis intensity vs. on-axis phase-shift for different ratios f between lens-diameter and beam-diameter.

the calculated phase-shift in the center of the film. This can be explained by the (more or less) strong anchoring of the first molecule-layers at the inner glass-surfaces and the resulting deformation gradient layer, which lowers the effective film-thickness. The strong influence of β is also shown in Figure 9. For normal incidence there is a clear threshold behaviour, whereas the threshold disappears at $\beta \geq 10$ deg. The experimental threshold has been measured to be $I_{th} = 395$ W/cm^2 in good agreement with the theoretical value calculated with the parameters $\epsilon_a = 0.62$, $K = 8 \cdot 10^{-12}$N,[9] $\beta = 0$, $d = 120\ \mu m$, $w_o = 170\ \mu m$.

Another experimental result is shown in Figure 10 where we measured the angle of maximum divergence of the diffraction pattern (i.e. the diameter of the outermost

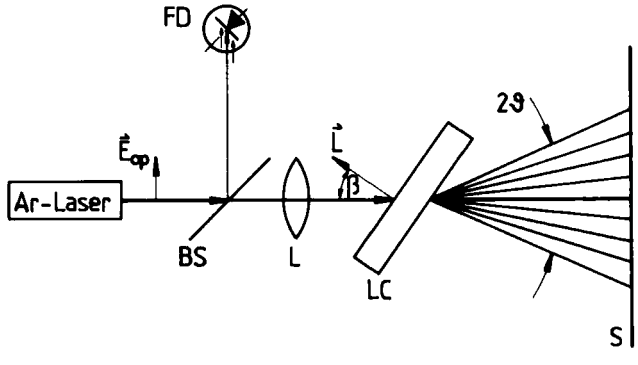

FIGURE 8 Experimental setup. E_{op}: Optical field, BS: Beam-splitter, FD: Calibrated foto-diode, L: Lens, LC: Liquid-crystal, L: Director, S: Screen.

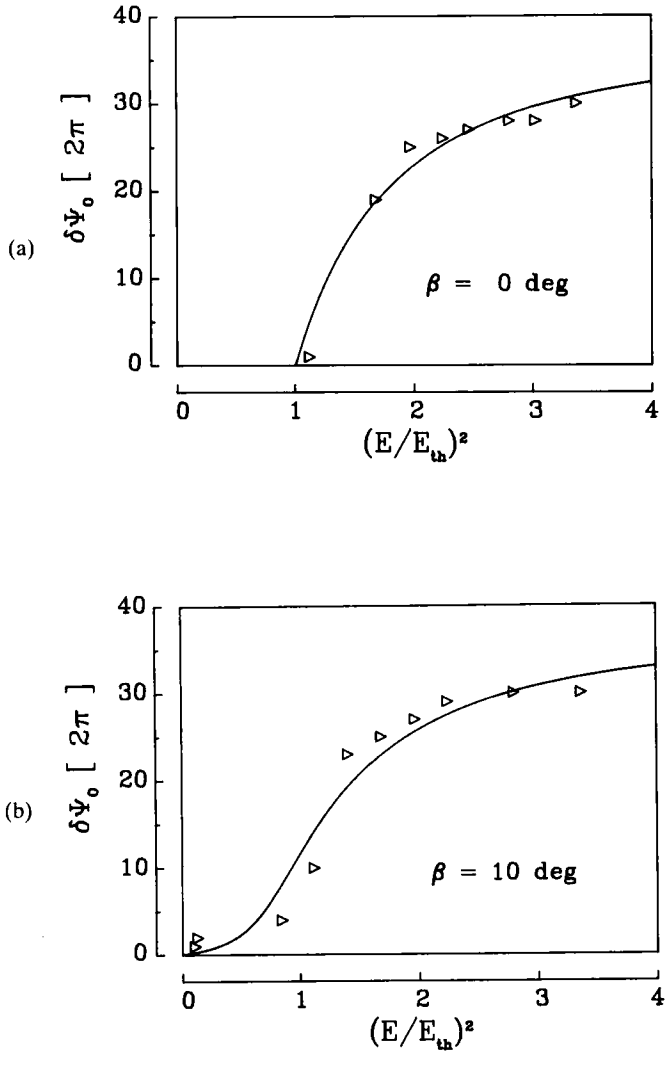

FIGURE 9 Number of observed diffraction-rings N vs. laser-intensity (experimental points) compared with the calculated on-axis phase-shift with respect to the relation $N = \delta\psi_o/2\pi$ for $\beta = 0$ deg (a), $\beta = 10$ deg (b), $\beta = 45$ deg (c).

ring) depending on the induced phase-shift or the total number of rings respectively. The theoretical curve is obtained by extrapolating ϑ-values calculated from Equation 26 for $\partial\Psi_o \leq 12\pi$. Even an extrapolation of this curve up to $\partial\Psi_o = 60\pi$ leads to good agreement between experimental data and shows a slightly quadratic dependence between the divergence-angle and the number of diffraction-rings instead of a simple linear relation as expected in geometrical-optic considerations.[11]

To investigate the dynamics of the reorientation and the related self-diffraction

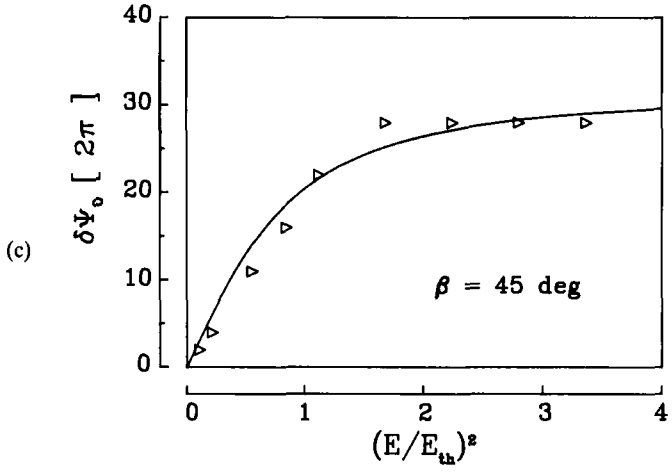

FIGURE 9 *(continued)*

effects we measured the on-axis intensity with a photo-diode placed behind a 5 μm-pinhole at a distance Z behind the film as a function of time. Results are given in Figure 11. The optical excitation has been stepwise (see Equation 13) and we chose $\beta \approx 0$. No remarkable changes in the on-axis intensity can be observed in this case for long times as 90 seconds after switching on the laser, i.e. no defocussing occurs during this time. After this 'delay-time' self-diffraction starts and the on-axis intensity decreases and oscillates. Each oscillation is accompanied by the appearance of an additional diffraction-ring. The theoretical curve has been calculated from Equation 26 by setting $\rho = 0$ and $f = 0.9$ (i.e. the phase-profile's diameter is somewhat smaller than the beam-waist) whereas the dynamics of the reorientation

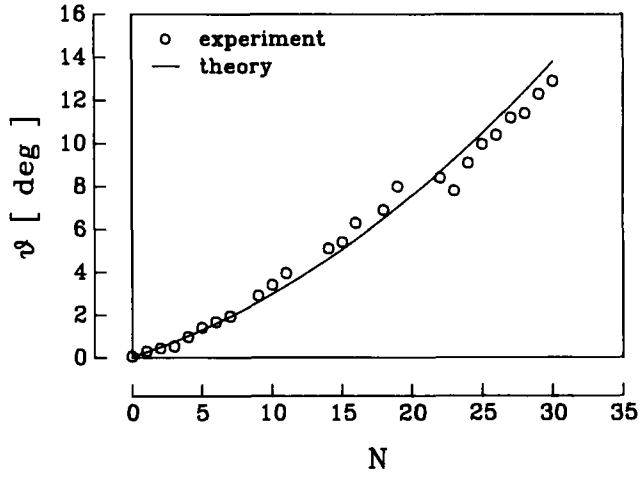

FIGURE 10 Diffraction-angle of the outermost ring vs. total number of observed rings.

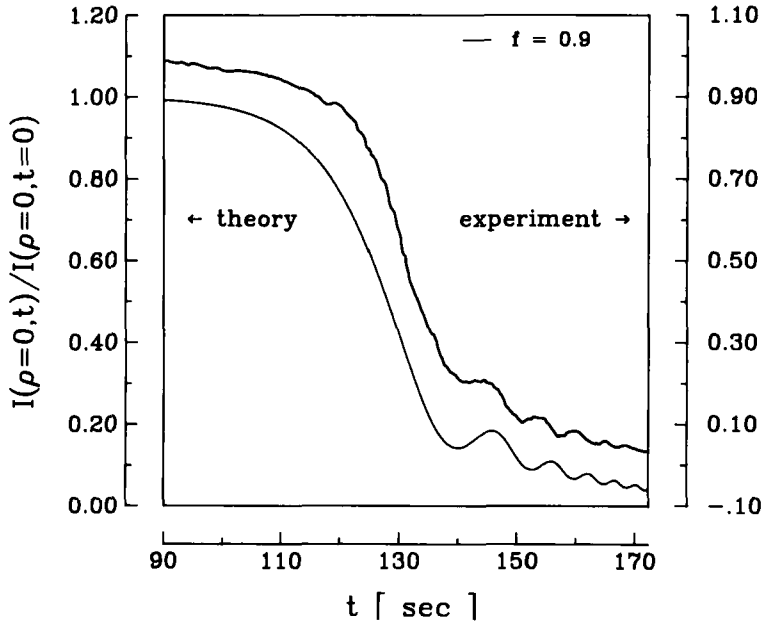

FIGURE 11 Dynamics of the on-axis intensity for a stepwise excitation at $t = 0$. $I_{th} = 520 W/cm^2$, $I = 890 W/cm^2$, $d = 120 \mu m$, $T = 25°C$, $\beta = 3{,}6 \cdot 10^{-4}$, $\gamma = 0{,}085 kg/ms$.

process has been considered as described in Equation 18. The same dynamics are shown in Figure 12 for another experiment where we display the number of the observed first 6 diffraction-rings as a function of time. As we pointed out above we have a long 'delay'-time compared with the reorientation time-constant. The 'delay'-time depends on the initial alignment related to the optical field (here

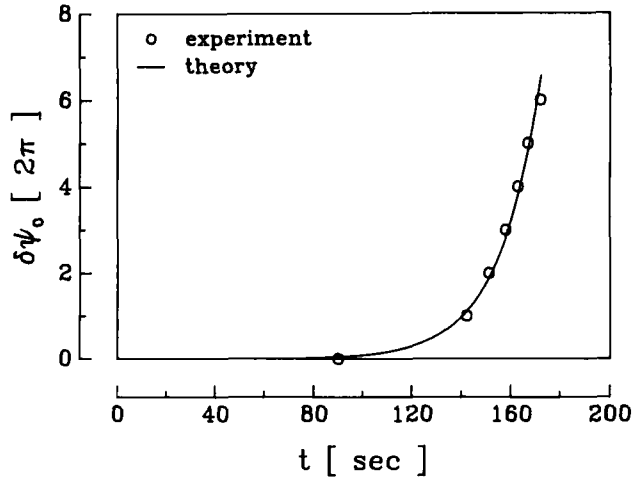

FIGURE 12 Number of observed diffraction-rings vs. time for a stepwise optical excitation at $t = 0$, same conditions as in Figure11.

expressed by the angle of incidence β). For $\beta = 0$ (exactly!) it should be impossible to reorient the director in finite times, but this would never be the case in a real experiment, because of weak anchoring or small fluctuations of the molecules around the initial alignment. The experimentally observed dynamics can be explained by our reorientation model if we assume $\beta = 3.6 \cdot 10^{-4}$ rad. The measured time-constant of $\tau = 17$s can be calculated with the experimental parameters $I = 890$ W/cm^2, $I_{th} = 520$ W/cm^2, $d = 120$ μm, $w_o = 47$ μm and $\epsilon_a = 0.62$, if we assume $K = 8 \cdot 10^{-12}$N and a viscosity of $\gamma = 0.085$ kg/ms in good agreement with Reference[12].

CONCLUSION

The strong self-diffraction and self-defocussing effects which can be observed with low power cw-lasers in nematic liquid-crystals have been modeled quantitatively. The model uses a simple diffraction theory, where the distortion of the laserbeam at a self-induced lens is described in terms of Gaussian beam optics, and a model of light-induced reorientation as a nonlinear mechanism in liquid crystals. The resulting diffraction pattern for various experimental parameters, e.g. the incident laser-intensity or the angle of incidence, can be calculated as well as the dynamics of self-defocussing. Experimental data have been presented to prove our model. The agreement between theory and experiment is good, though we simply approximated the induced phase-profile by a gaussian lens. Consideration of the exact shape of the phase-profile should lead to further improvement of such models.

Financial support from the Deutsche Forschungsgesellschaft is gratefully acknowledged. Liquid Crystals were kindly supplied by BDH Chemicals and Hoffmann La Roche.

References

1. Y. R. Shen, "The Principles of Nonlinear Optics", Wiley, New York 1984.
2. A. S. Zolot'ko *et al.*, *JETP Lett.*, **32**, 155 (1980).
3. I. C. Khoo and P. Normandin, *Optics Letts.*, **9**, 285 (1984).
4. I. C. Khoo, *IEEE J. Quant. Electron.*, **QE-22**, 1268 (1986).
5. L. Csillag *et al.*, *Mol. Cryst. Liq. Cryst.*, **84**, 125 (1982).
6. M. Abramowitz and A. Stegun, "Handbook of Mathematical Functions", Dover Publc. New York (1972).
7. I. C. Khoo, T. H. Liu and R. Normandin, *Mol. Cryst. Liq. Cryst.*, **131**, 315 (1985) and I. C. Khoo, T. H. Liu and P. Y. Yan, *J. Opt. Soc. Am. B*, **4**, 115 (1987).
8. I. C. Khoo *et al.*, *J. Opt. Soc. Am. B*, **4**, 886 (1987).
9. D. Weaire, B. S. Wherrett, A. B. Miller and S. D. Smith, *Optics Letts.*, **4**, 331 (1979).
10. Bradshaw, Raynes, Bunning and Faber, *J. Physique*, **46**, 1513 (1985).
11. S. D. Durbin, S. M. Arakelian and Y. R. Shen, *Optics Letts.*, **6**, 411 (1981).
12. H. Kneppe, F. Schneider and N. K. Sharma, *J. Chem. Phys.*, **77**, 3203 (1982).